



Neuroradiology/Head and Neck Imaging *Review Article*

## Imaging of Non-atherosclerotic Vasculopathies

Amit Agarwal<sup>1</sup>, Girish Bathla<sup>2</sup>, Sangam Kanekar<sup>3</sup>

<sup>1</sup>Department of Radiology, University Texas Southwestern, Dallas, Texas, <sup>2</sup>Department of Radiology, University of Iowa, Iowa City, Iowa, <sup>3</sup>Department of Radiology, Penn State Health, Hershey, Pennsylvania, United States.



**\*Corresponding author:**

Amit Agarwal,  
Department of Radiology,  
University Texas Southwestern,  
5323 Harry Hines, Dallas  
75390, Texas, United States.

[amitmamc@gmail.com](mailto:amitmamc@gmail.com)

Received : 07 June 2020  
Accepted : 12 September 2020  
Published : 13 October 2020

DOI  
10.25259/JCIS\_91\_2020

Quick Response Code:



### ABSTRACT

Non-atherosclerotic vasculopathies (NAVs) may present with various neurological symptoms ranging from headache, stroke, visual symptoms, and various types of intracranial hemorrhage. NAVs result from different etiologies which include collagenopathies, immunological, hematological, and infection mechanisms, and other rarer unidentifiable or idiopathic causes. NAV etiologies account for about 10–15% and 20–25% of adult and pediatric stroke cases, respectively, and therefore, diagnosing the underlying cause of NAV becomes clinically very important. Clinical diagnosis of NAV is challenging because the clinical presentation is very non-specific and overlapping with various other central nervous system disorders. Before the advent of non-invasive techniques, making a diagnosis of non-atherosclerotic vasculopathy as a cause of the stroke was very challenging. Today with newer techniques such as high-resolution magnetic resonance (MR), MR and computed tomography perfusion, and angiogram, there are number of pointers which can give us a lead about the non-atherosclerotic causes. Imaging may provide the first lead to the clinician regarding the diagnosis or possible differential diagnosis so that the targeted and focused biomarkers (blood, cerebrospinal fluid, or/and in some cases biopsies) may be obtained to clinch the diagnoses. The purpose of the article is to enumerate the causes, clinical features, and illustrate the imaging findings of the various non-atherosclerotic vasculopathic disorders and discuss “pearls” to their diagnosis. In this article, we have also discussed the latest advances in vascular imaging and elaborated on few uncommon non-atherosclerotic vasculopathies. These are very relevant clinically in the day-to-day practice for the radiologist, neurologist, and the neurointerventionalist.

**Keywords:** Vasculopathy, Angiogram, Computed tomography angiography, Magnetic resonance angiography

### INTRODUCTION

Non-atherosclerotic vasculopathies (NAVs) may result from various systemic or local etiologies, which include collagenopathies, immunological, hematological, hereditary, infection mechanisms, and idiopathic causes. NAV disorders can affect all the age groups childhood, middle age, and elderly patients. It may present with variety of neurological symptoms such as headache, neck pain, visual symptoms, hemorrhagic and non-hemorrhagic strokes, mono or hemiplegia, or myelopathy. NAV is a common cause of stroke in young adults and adolescents with arterial dissection accounting for approximately 2% of all ischemic strokes but about 20% of strokes in the young and middle aged.<sup>[1,2]</sup> Making a specific diagnosis of the underlying cause of NAV is clinically very challenging because of the non-specific clinical presentation.

Cross-sectional imaging, especially magnetic resonance (MR), plays a key role in the diagnosis of NAV. Documentation of the corroborative findings in the brain parenchyma on MR and vessel changes on magnetic resonance angiography (MRA) or computed tomography angiography

This is an open-access article distributed under the terms of the Creative Commons Attribution-Non Commercial-Share Alike 4.0 License, which allows others to remix, tweak, and build upon the work non-commercially, as long as the author is credited and the new creations are licensed under the identical terms.

©2020 Published by Scientific Scholar on behalf of Journal of Clinical Imaging Science

(CTA) may support the diagnosis and the underlying cause of the disease. MR is very sensitive for identifying brain parenchymal changes, which mainly consist of small or medium size infarcts and/or microhemorrhages. CTA and MRA are very sensitive for detecting changes in the larger and medium size vessels, especially in the carotids, vertebral, and vessels around the circle of Willis. However, both these modalities lack the intrinsic resolution to diagnose the changes in smaller and tertiary branches. In these cases, conventional angiography remains the gold standard. Conventional angiogram shows non-specific findings such as occlusion and irregular narrowing, alternating with dilation and sometimes aneurysm. However, distribution and site of the vessels involved along with various parenchymal findings on imaging helps in documenting the cause and effects of many of these disorders.

High-resolution MR vessel wall imaging (VWI) is a relatively new imaging technique, which is increasingly being used across multiple centers for the evaluation of patients with suspected vasculitis and other cerebral vascular diseases such as arterial dissection, intracranial atherosclerosis, and for better characterization of aneurysms. This is usually performed in conjunction with routine time-of-flight (TOF) MR angiography and involves obtaining high-resolution 3D images with “black-blood technique.” Images are acquired using high spatial and high contrast resolution techniques, preferably on a 3T magnet, usually with and without contrast. The most common indication for VWI is vasculitis (primary or secondary) with other less common indications including intracranial dissection, defining complex aneurysms, and better characterization of atherosclerotic changes. Intracranial atherosclerotic disease is defined by eccentric wall thickening, with or without enhancement, with widespread involvement of the large vessels such as distal internal carotid artery (ICA) and vertebral arteries. Vessel wall thickening is usually concentric in vasculitis with enhancement almost universally seen. Imaging response to steroid is often seen in vasculitis and expectedly absent with atherosclerotic disease. Intracranial dissection is characterized by eccentric wall thickening and enhancement with the presence of intimal flap and/or intramural thrombus. VWI is also helpful in characterization of intracranial atherosclerotic plaques, differentiation of vasculitis from reversible cerebral vasoconstriction syndrome (RCVS), and for equivocal causes of vascular narrowing.

In this article, we discuss the common causes, classification of non-atherosclerotic vasculopathy affecting the central nervous system (CNS) [Table 1] and imaging findings of various disease entities, discuss “pearls” to their diagnosis, and highlight how to differentiate between the common NAVs.

**Table 1:** Common causes of non-atherosclerotic vasculopathy.

Arterial dissections Fibromuscular dysplasia Dilatative arteriopathy (dolichoectasia) Cerebral amyloid angiopathy Heritable disorders of connective tissue Pseudoxanthoma elasticum (PXE) Ehlers-Danlos syndrome Marfan's syndrome CNS vasculitides [Table 2] Systemic vasculitides Polyarteritis nodosa Allergic angiitis Granulomatosis (Churg-Strauss syndrome) Hypersensitivity vasculitis, Wegener's granulomatosis Overlap syndromes Thrombotic thrombocytopenic purpura CADASIL Sickle cell disease Moyamoya syndrome Arteritis caused by infections Bacterial Fungal infections Viral infections Parasitic infections Radiation-induced vasculitis Vasculopathy in drug abusers Reversible cerebral vasoconstriction syndrome (includes drug-induced vasculopathy)
CADASIL: Cerebral autosomal dominant arteriopathy with subcortical infarcts and leukoencephalopathy

## BODY OF ARTICLE

### Arterial dissections

Cervical artery dissection is the most common non-atherosclerotic cause of stroke in young adults, accounting for 20% of all ischemic strokes and 27% of brainstem and cerebellar infarctions.<sup>[3,4]</sup> Cervical artery dissection can be either traumatic or spontaneous in origin. Traumatic dissection is a complication of severe blunt head-and-neck trauma. Spontaneous arterial dissection can be without any discernible cause or secondary to underlying arteriopathy (an extracellular matrix defect), leading to weakness of the vessel wall predisposing it to dissection. The associated intrinsic arteriopathies with dissection include fibromuscular dysplasia, Marfan syndrome, Ehlers-Danlos IV syndrome, and cystic medial necrosis.

Spontaneous cervical artery dissections involve the ICA in 68% of cases, the vertebral artery (VA) in 27%, and both in 5%.<sup>[4]</sup> It most commonly affects the ICA, 2–3 cm distal to the carotid bifurcation, and tends not to extend beyond the petrous portion.<sup>[5]</sup> Craniocervical arterial dissection is

initiated by tearing of the vessel wall between the intima and media or adventitial lining of the vessel. Secondary to high pressure, blood penetrates the endothelial cells of the tunica intima and penetrates the media layer with creation of a false lumen with intramural hematoma [Figure 1a and b]. This results in stenosis or occlusion of the true lumen, often with thrombus formation and thromboembolic event. The sudden tapering and severe narrowing/occlusion of the cervical ICA just beyond its origin, gives it a “flame” like shape, and is considered as one of the classic appearances of cervical carotid dissection [Figure 1c and d]. Subadventitial dissection results in formation of pseudoaneurysm.<sup>[6-8]</sup> Carotid artery dissections usually present with ipsilateral neck pain or headache, partial or complete Horner’s and ischemic stroke.

The extracranial VA is the second most commonly affected artery. VA dissection is most common in the atlas loop (V3 segment) at C1-C2 level.<sup>[5]</sup> The most common clinical presentation of VA dissection is headache or neck pain, followed by posterior circulation ischemia.<sup>[5,9]</sup> Intracranial dissection, usually of the vertebrobasilar arteries, is being increasingly recognized over the last few years. Recent studies have reported a higher prevalence of intracranial dissection than that of extracranial cervical dissection. Intracranial arterial dissection is less common than cervical artery dissection in adults of European ethnic origin, however, recent studies suggest preponderance of intracranial artery dissection in children and in the Asian populations. Apart from the demographic difference, the

higher incidence in recent literature could be secondary to recent advanced imaging techniques. The most common clinical presentation is headache followed by posterior circulation ischemic symptoms. Subarachnoid hemorrhage (SAH) is uncommon.<sup>[10,11]</sup>

Imaging plays an important role in the diagnosis of dissection. Three common patterns of dissection seen on CTA/MRA include long segment lumen narrowing, acute occlusion, and distal pouch. Acute dissection on CTA is seen as a narrow eccentric lumen with an increase of the external diameter of the artery. The typical target sign of narrow eccentric lumen surrounded by crescent-shaped mural thickening and thin annular enhancement is very specific for dissection but less sensitive.<sup>[12,13]</sup> Other signs of arterial dissection on CTA include intimal flap, dissecting aneurysm, and parenchymal complications such as stroke [Figure 2].

In addition to routine MRI of the brain and MRA of head and neck, axial fat-saturated T1 and/or PD are important for the diagnosis of dissection. Identification of intramural hematoma can be challenging on routine TOF MR angiograms due to flow signal from the true lumen. Dissection protocol sequences include T1-weighted fat-suppression spin-echo sequence with no fat or flowing blood signal and superior demarcation of the false lumen from the true lumen, especially during the subacute phase when the intramural hematoma is bright on T1.<sup>[14]</sup> The most common MRI finding of dissection is crescent-shaped intramural hematoma, which can be easily distinguished from the

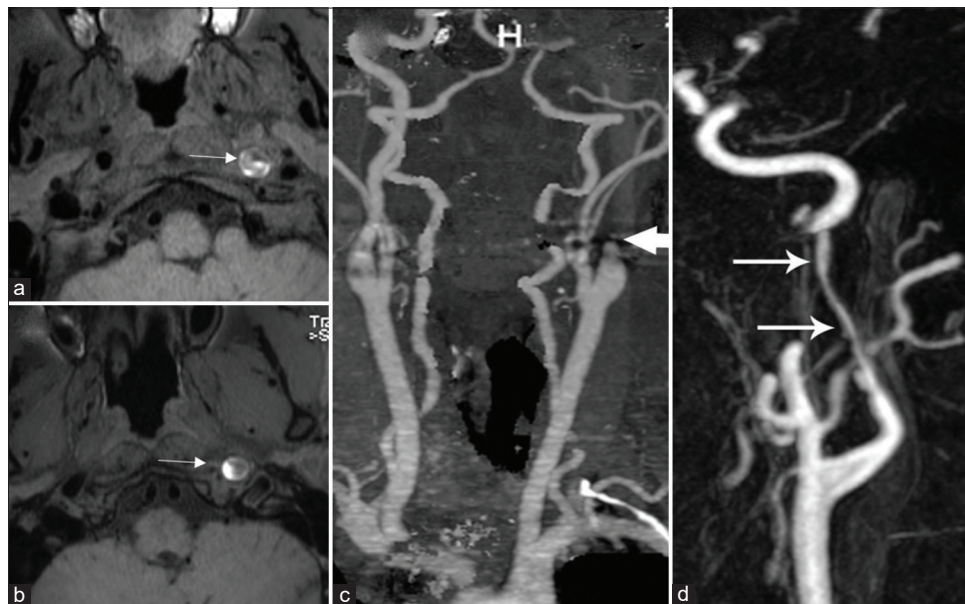


**Figure 1:** Imaging appearances of dissection. Intramural thrombus: (a and b) Axial T1-weighted image shows decrease normal flow void (arrowhead) in the left ICA surrounded by a crescentic T1 hyperintense mural hematoma (arrow). Acute occlusion: (c) Contrast-enhanced MRA of the neck demonstrates flame like dissection (arrow) of the left ICA with complete occlusion of the lumen. (d) Contrast-enhanced MRA neck shows severe tapering (arrows) of the left ICA due to dissection.

surrounding tissue on fat-suppressed T1-weighted images, especially during the subacute phase when the hematoma shows bright T1 signal [Figure 1a]. The hematoma shows signal intensity depending on the stage of the hematoma and the products of hemoglobin breakdown.<sup>[15]</sup> Routine MRI along with MR angiography has excellent sensitivity and specificity for cervical arterial dissection, usually in the range of 80–98%.<sup>[16]</sup> Conventional MR imaging is not as helpful in diagnosis of VA dissection because of the flow-related enhancement in the venous plexus of the foramen transversarium. However, with the addition of dissection protocol fat-sat T1 sequences along with the relatively new VWI techniques, MRI has become the imaging modality of choice for extracranial as well as intracranial arterial dissection. Contrast-enhanced VWI sequences can reveal eccentric or circumferential enhancement representing inflammation or changes secondary to stagnant blood within the false lumen. Extensive enhancement might predict higher chance for recurrent and multiple dissections. Digital subtraction angiography, although still considered as gold standard, is sparingly used at present. The angiographic hallmark of cervical carotid dissection is long, tapered, usually eccentric narrowing of the carotid distal to the bulb, referred to as the “string sign.”<sup>[17-19]</sup>

### Fibromuscular dysplasia (FMD)

FMD is a non-atherosclerotic, non-inflammatory vascular disease affecting medium to large-sized vessels. It is far more prevalent in females than in males. Depending on histology, FMD is divided into the medial, intimal, and periarterial or subadventitial forms. The medial or muscular dysplasia occurs in 90–95% of cases.<sup>[20]</sup> The less common intimal variant of FMD can present as linear shelf-like filling defect,



**Figure 2:** A 41-year-old male patient with acute-onset right hemiplegia due to spontaneous left ICA dissection. Axial source image from CTA shows dissection flap in the left carotid artery (arrowhead).

usually along the posterior wall of the carotid bulb with high risk for recurrent strokes. FMD usually involves the cervical portion of the ICA, starting distal to the bifurcation and extends up to the level of C1. Bilateral ICA involvement is common, occurring in 86% of patients with FMD. About 20% of patients with ICA FMD may have coexisting VA FMD. The incidence of intracranial aneurysms in patients with cervical FMD is around 20–50%. Other associations include spontaneous carotid artery dissection, extracranial aneurysm, and spontaneous arteriovenous fistulas. Clinically, carotid bruits are present in 70–100%.

CTA/MRA shows three patterns of FMD. Constricting bands composed of fibrous dysplastic tissue and proliferating smooth muscle cells in the media alternating with areas of luminal dilatation related to medial thinning and disruption of the elastic membrane give rise to the characteristic “string-of-beads” appearance on arteriography [Figure 3]. This pattern is usually associated with the medial histologic type and is present in approximately 80% of cases. Less common patterns show a smooth concentric tubular lesion or an eccentric outpunching that may progress to an aneurysm. The intimal variant FMD (carotid webs) is best seen on the sagittal plane of CT angiogram and are often bilateral.<sup>[21-25]</sup>

### Dilatative arteriopathy (dolichoectasia [DE])

DE is a common dilatative arteriopathy that is defined as an elongation or widening of the intracranial arteries, mainly involving vertebral and basilar arteries. The prevalence of DE ranges from 0.06% to 5.8%. The exact pathogenesis of intracranial arterial DE is still unclear. Multiple physiological processes can contribute, however, systemic arterial

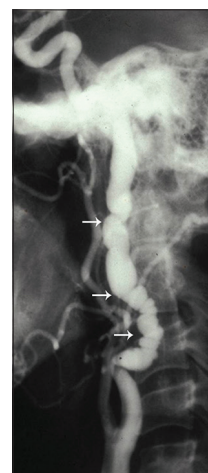


**Figure 3:** Fibromuscular dysplasia. A 42-year-old woman presented with transient ischemic attacks. Conventional angiogram of the neck shows the “string and pearl” sign in the internal carotid artery consistent with fibromuscular dysplasia. Beaded appearance with multiocal areas of apparent narrowing (white arrows) noted.

hypertension is the most commonly implicated underlying cause. This is further supported by histopathological studies which reveal degeneration of the internal elastic lamina and thinning of the media secondary to prolonged systemic hypertension.<sup>[26,27]</sup>

Most cases are asymptomatic; however, DE can produce symptoms due to direct compression of brain stem and cranial nerves.<sup>[26]</sup> The most important clinical presentations of DE include acute ischemic symptoms and compressive cranial neuropathy [Figure 4a and b]. Compression of the V and VII cranial nerves may cause trigeminal neuralgia and hemifacial spasm, respectively. Hydrocephalus is a rare complication of DE seen due to compression of the foramen of Monro, 3<sup>rd</sup> ventricle, or cerebral aqueduct. Very rarely, a fatal outcome may be seen due to vascular rupture.

Routine CT brain can demonstrate DE as a tortuous, slightly hyperdense, elongated vertebrobasilar artery. MRI with FIESTA or CISS sequence or source images of TOF MRA is more sensitive in demonstrating the dilatation as well as mass effect on surrounding brain parenchyma and cranial nerves. Radiographic criteria for the diagnosis of vertebrobasilar DE include diameter >4.5 mm in any location along its course, lateral deviation >10 mm perpendicular to a straight line joining its origin to its bifurcation, origin at the level of the pontomedullary junction, bifurcation above the suprasellar cistern, lateral to the margin of the clivus or dorsum sellae, and basilar length >29.5 mm or intracranial VA length >23.5 mm. Identification of fusiform aneurysm and/or thrombus is not uncommon.<sup>[28]</sup>

### Cerebral amyloid angiopathy (CAA)

CAA is a cerebrovascular disorder characterized by the deposition of  $\beta$ -amyloid protein in the media and adventitia of small and medium-sized vessels of the cerebral cortex, subcortex, and leptomeninges.<sup>[29]</sup> The amyloid deposition is most prevalent in the parietal and occipital lobes vessels

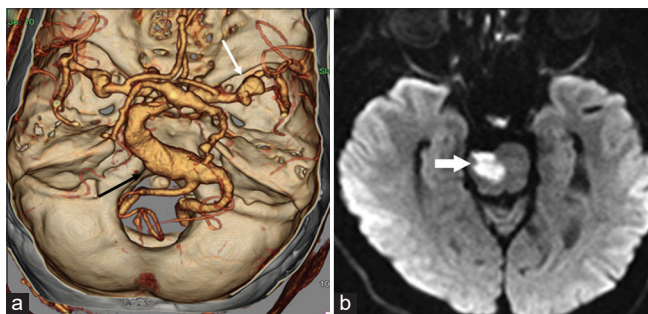


**Figure 4:** Dolichoectasia with pontine infarction in a 71-year-old male patient. (a) Reformatted MPR image of the intracranial CTA shows dolichoectasia of the vertebrobasilar artery with fusiform aneurysm of the vertebral artery (black arrow). Note is also made of the dysplastic middle cerebral arteries and aneurysms at the bifurcation (white arrow). (b) Axial DWI image shows acute stroke on the right side of the pons (arrow).

while the deep gray and white matters are spared. There is progressive destruction of smooth muscle cells, with sparing of the endothelium. These changes in the vessel wall are associated with fibrinoid necrosis, focal vessel wall fragmentation, and microaneurysms, predisposing to hemorrhage. Affected vessels become rigid and fragile and in late stages assume a rounded or “double-barrel contour” on histopathology.<sup>[30]</sup> Changes in the wall lead to luminal narrowing which, in turn, lead to transient ischemic attack (TIA), and ischemic change, which collectively leads to dementia. It is most commonly seen in elderly population with age more than 65 years. Inflammatory CAA is the less common form, which is further classified into CAA-related inflammation (CAA-RI) and CAA-related angiitis. The distinction between the two forms of inflammatory disease is pathological and cannot reliably be made on imaging. Inflammatory changes in CAA-RI are usually perivascular with variable degree of parenchymal edema presenting with headaches, seizures, and mental status changes. CAA-related angiitis is a transmural angi destructive process often secondary to granulomatous infiltrate.

Susceptibility-weighted imaging-gradient-echo sequences (SWI/GRE) have revolutionized the diagnosis of CAA. SWI-GRE images often show multiple, small, old hemorrhages as tiny signal drop outs due to hemosiderin. Microhemorrhages (<5 mm) are generally asymptomatic and are characteristically distributed in the cortical-subcortical region.<sup>[27]</sup> Large intracerebral hemorrhage (>5 mm) is often symptomatic and may manifest as headaches, focal neurologic deficits, or seizure. They may be associated with subarachnoid or subdural hemorrhage. CT scan is insensitive to microhemorrhages. On MRI, cortical-subcortical intraparenchymal hemorrhages on the background of diffuse white matter T2 hyperintensity and cortical atrophy in elderly patients should raise the suspicion for CAA [Figure 5a and b].<sup>[30]</sup> The Modified Boston criteria uses a combination of clinical, radiological and pathological parameters. Although imaging can suggest probable or possible CAA, the definitive diagnosis is only made with pathology on autopsy. Classic MRI findings include lobar, cortical, or cortical-subcortical hemorrhages and superficial siderosis without another underlying cause. The cerebral white matter may show changes of leukoencephalopathy, which appears as low attenuation of white matter on CT or high signal intensity on T2-weighted imaging. These changes are due to the combination of demyelination, ischemia, infarction, and edema. CAA-RI classically presents with varying degree of subcortical edema with frequent involvement of the adjacent cortex and leptomeninges. Subcortical edema is usually reversible and responsive to immunosuppressive treatment. Circumferential thickening and enhancement of the vessel wall is often seen in the inflammatory variants of CAA, in a pattern similar to primary angiitis of the CNS (PACNS).

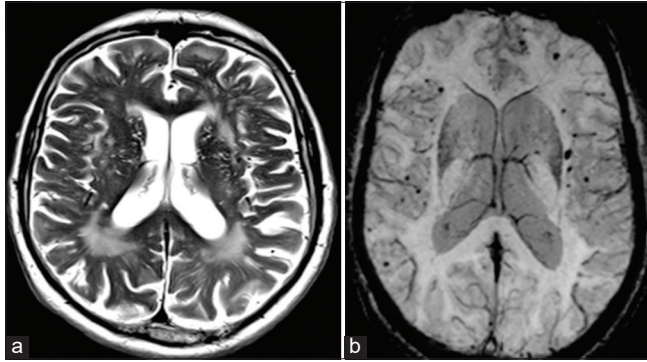


**Figure 5:** Amyloid angiopathy. A 74-year-old male patient presented with dementia. (a) Axial T2-weighted fast spin-echo MR image does generalized prominence of convexity sulci and patchy T2 hyperintensity in the cerebral white matter. (b) Axial SWI MR image shows multiple foci of signal loss in cortical-subcortical locations, consistent with chronic microhemorrhages.

### Heritable disorders of connective tissue

A variety of hereditary connective tissue disorders involves the skin, vascular system, and skeletal tissues and discussing all of them is beyond the scope of this article. We discuss the most clinically relevant disorders: Ehlers-Danlos syndrome and Marfan's syndrome.

Ehlers-Danlos syndrome is a heritable connective tissue disorder characterized by skin hyperextensibility, fragile and soft skin, delayed wound healing, easy bruising, and generalized joint hypermobility. About 50% of patients with classic Ehlers-Danlos syndrome harbor mutations in the COL5A1 and the COL5A2 gene, encoding the 1- and the 2-chain of type V collagen, respectively.<sup>[31]</sup>

The diagnosis of EDS is established by clinical examination and family history. Cardiac lesions are common, which include mitral and tricuspid valve prolapse, septal defects, and dilatation of the aortic root and pulmonary arteries.<sup>[32]</sup> The most important and frequent cerebrovascular complications are carotid-cavernous fistulas due to ruptured aneurysm and arterial dissections. Extra- and intracranial aneurysms have also been reported. Rupture of various systemic and cerebral vessels leads to frequent bleeding and SAH [Figure 6a-d]. Conventional angiography and angioplasty have a high rate of complications, and therefore, non-invasive techniques like MRA are primary investigation of choice in patients with Ehlers-Danlos syndrome.<sup>[33]</sup>

Marfan's syndrome is more common than other hereditary disorders with an incidence rate of approximately 4–6/100,000 individuals. The condition is inherited as a dominant trait. A gene defect is located on the long arm of chromosome 15, resulting in a mutation of the FBN1 gene that encodes fibrillin-1.<sup>[34,35]</sup>

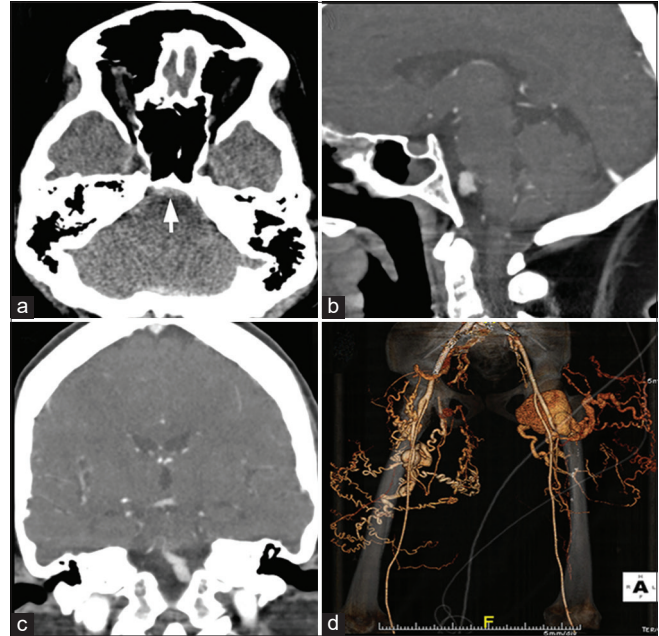


**Figure 6:** A 36-year-old female with Ehlers-Danlos syndrome presented with severe headache. (a) CT scan of the head shows prepontine subarachnoid hemorrhage (arrow). (b and c) Prior CT angiogram of the brain depicted a complex saccular fusiform aneurysm at the vertebrobasilar confluence which has been stable over many years. (d) CTA of the lower extremities shows large tuft of coiled, vessels, complex pseudoaneurysm, and arteriovenous fistula arising from the proximal deep femoral artery bilaterally.

It has a broad continuum of clinical manifestations involving the ocular, skeletal, and cardiovascular systems.<sup>[30]</sup> Lens dislocation, seen in about 60%, is a hallmark feature. Myopia, retinal detachment, glaucoma, and early cataract formation are other ocular manifestations. The vascular abnormalities relate to abnormal collagen and elastin. Aortic regurgitation due to aortic root dilatation, mitral valve prolapse, aortic aneurysms, and dissections is common vascular complications. Carotid and VA dissections have also been reported.<sup>[35,36]</sup> Most of the cerebrovascular events in Marfan syndrome relate to the cardiac and aortic manifestations. CTA or MRA of the chest and neck are very sensitive in the diagnosis of dissection and show the extent of flap, luminal narrowing, and aneurysm if associated [Figure 7].

### CNS vasculitis

The vasculitides encompass a heterogeneous group of disorders pathologically characterized by inflammation of the blood vessel wall. Chapel Hill Consensus Conference 2012 revised the International Nomenclature of Vasculitides depending on the size of the vessel involved [Table 2].<sup>[37]</sup> CNS vessels may be involved in process of (a) primary systemic disorder such as giant cell arteritis (GCA) and polyarteritis



**Figure 7:** A 51-year-old male patient with Marfan’s syndrome with multiple TIAs. Axial image from chest CTA reveals dissection in the arch and descending aorta (arrows). Dissection is also seen extending into the right brachiocephalic artery (arrowhead).

nodosa; (b) secondary vasculitis, where the CNS blood vessels are affected secondary due to collagen vascular diseases, infections, tumors, and substance abuse; or (c) due to idiopathic form of vasculitis limited to the brain and spinal cord known as PACNS.

Vasculitis is a rare yet potentially treatable cause of stroke, but the diagnosis of vasculitis as a cause of stroke can be challenging. Brain and meningeal biopsy till date remain the gold standard for diagnosis. Vasculitis shows patchy rather than contiguous involvement and therefore non-lesional leptomenigeal biopsies may not confirm the diagnosis of CNS vasculitis. The most important clinical dilemma is the risk and the practicality of subjecting the suspected cases of vasculitis to brain biopsy, which is negative in up to half of patients. Therefore, imaging remains the primary investigation in such patients and plays a key role in diagnosing the parenchymal complications and at times pointing toward the specific cause of the vasculitis.

Imaging findings can be divided largely into two categories: Parenchymal changes due to effect and vascular changes due to cause. The typical MR findings include multiple non-specific T2 hyperintense lesions involving white matter (deep as well as the subcortical), the cortex, and deep gray matter nuclei. These changes may mimic various other focal white matter lesions such as multiple sclerosis, Lyme’s, and sarcoidosis. In addition to the T2 hyperintensities, MRI scans may also show single or multiple territorial infarcts on T2 and DWI depending on the stage of infarct. Multiple subacute or chronic microhemorrhages are identified on SWI/GRE images.

CTA and MRA are sensitive in demonstrating the vasculitis changes in the neck and around the circle of Willis. Both

**Table 2:** Names for vasculitides adopted by the 2012 International Chapel Hill Consensus Conference on the Nomenclature of Vasculitides.

Large vessel vasculitis
Giant cell arteritis
Takayasu arteritis
Idiopathic aortitis (IgG-4)
Medium vessel vasculitis
Polyarteritis nodosa
Kawasaki disease
Small vessel vasculitis
Antineutrophil cytoplasmic antibody-associated vasculitis
Microscopic polyangiitis
Granulomatosis with polyangiitis (Wegener)
Eosinophilic granulomatosis with polyangiitis (Churg-Strauss)
Immune complex vasculitis
Anti-glomerular basement membrane disease
Cryoglobulinemic vasculitis
IgA vasculitis (Henoch-Schönlein)
Hypocomplementemic urticarial vasculitis (anti-C1q vasculitis)
Variable vessel vasculitis
Behcet disease
Cogan syndrome
Single-organ vasculitis
Cutaneous leukocytoclastic angiitis
Cutaneous arteritis
Primary central nervous system vasculitis
Isolated aortitis
Vasculitis associated with systemic disease
Lupus vasculitis
Rheumatoid vasculitis
Sarcoid vasculitis
Vasculitis associated with probable etiology
Hepatitis C virus-associated cryoglobulinemic vasculitis
Hepatitis B virus-associated vasculitis
Syphilis-associated aortitis
Drug-associated immune complex vasculitis
Drug-associated ANCA-associated vasculitis
Cancer-associated vasculitis

these techniques, however, have a poor sensitivity and specificity for the distal vessels. Unfortunately, various vasculitic processes predominately involve only the distal vessels which require invasive procedures like catheter angiography for the diagnosis. The classic angiographic findings include multiple arterial occlusions and segmental stenosis, particularly of the small cortical vessels, sometimes separated by dilatations giving rise to a “beaded” appearance. Rarely, small aneurysms can also be visualized. Over the last decade, vessel wall MR imaging (VWI) has seen marked widespread increase in clinical applicability. The most commonly used protocol used for this includes a T1-weighted vessel wall sequence before and after intravenous gadolinium contrast along with suppression of blood signal using either spin-echo technique or utilization of spatial saturation

band. In fact, vasculitis is usually the most common clinical indication to get VWI done across most of the centers. Compared to conventional TOF MR angiogram, VWI offers great advantage in identification of non-stenotic lesions and to characterize vessel wall inflammation. However, catheter angiogram still remains the gold-standard imaging modality for the evaluation of vasculitis. A normal arteriogram does not exclude the presence of vasculitis. Angiographic changes of the primary and secondary vasculitides are similar.

## LARGE VESSEL VASCULITIS

### Giant cell (temporal) arteritis

GCA is a chronic vasculitis that affects large and medium-sized vessels usually involving the superficial cranial arteries. It affects patients older than 50 years of age, with an estimated annual incidence of 20/100,000.<sup>[38]</sup> The branches of the external carotid artery, especially the superficial temporal and occipital arteries, are most frequently involved. The ICA, extra-carotid VA, subclavian, coronary, femoral, and even intracranial arteries may also be affected.

Two-thirds of patients present with headache, often in association with musculoskeletal complaints. The other prominent clinical features include unilateral or bilateral blindness, cervical myelopathy, and TIAs.<sup>[39]</sup>

The erythrocyte sedimentation rate is typically increased to 100 mm/h or more. Ultrasonography of the affected vessel may show a “halo sign,” a hypoechoic circumferential wall thickening that occurs around the arterial lumen. Contrast-enhanced CTA/MRA may show severe irregularities, narrowing, and stenosis of the vertebral, and internal and external carotid arteries [Figure 8]. Contrast-enhanced high-resolution MRI shows areas of active inflammation and enhancement of the vessel wall.<sup>[38-40]</sup> Brain MRI may show few non-specific hyperintensities in the brain parenchyma on fluid-attenuated inversion recovery (FLAIR) images. [18F]-FDG PET, which can examine all of the involved vessels with a single examination, shows areas of abnormal vascular uptake typically synonymous with vessel wall inflammation. Temporal artery biopsy is necessary for establishing the diagnosis.

### Takayasu's arteritis

Takayasu arteritis/pulseless disease is a chronic granulomatous, large vessel, arteritis that primarily affects the aorta, its main branches, and the pulmonary arteries. It is most commonly seen in Japan, Southeast Asia, India, and South and Central American countries, including Mexico, Peru, and Brazil. Females make up 80–90% of patients, mostly in the second and third decades of life.<sup>[41]</sup> Takayasu arteritis is thought to be an inflammatory process due to a genetically predisposed immune response. It is characterized

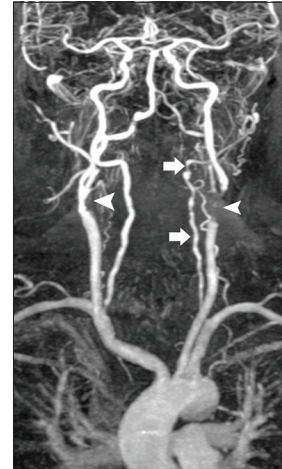


**Figure 8:** Giant cell arteritis. A 61-year-old male patient with temporal artery biopsy proven case of giant cell arteritis. Contrast-enhanced MRA of the neck shows severe irregularities, narrowing and stenosis of the left vertebral (arrow), bilateral internal carotid (arrowheads). There is complete occlusion of the left external carotid arteries.

by granulomatous inflammation and marked intimal proliferation and fibrosis of the medial and adventitial layers of the arterial wall, which eventually leads to stenosis, occlusion, and, occasionally, post-stenotic dilatations and aneurysm formation.

The clinical manifestations are divided into early and late phases. The early or prepulseless phase is characterized by nonspecific systemic features such as low-grade fever, malaise, weight loss, and fatigue. The late or occlusive phase is characterized by diminished or absent pulses, associated with limb claudication and blood pressure discrepancies, vascular bruits, hypertension (due to renal artery stenosis), mesenteric angina, and various cardiac symptoms. TIAs and ischemic stroke are reported in 10–20% of patients with Takayasu arteritis.<sup>[42]</sup>

The clinical presentation and laboratory tests are often nonspecific; therefore, imaging plays a key role in the diagnosis. Doppler ultrasonography may show circumferential vessel wall thickening. Cross-sectional imaging with CT MRI and MRA demonstrates mural thickening, luminal narrowing, and luminal dilatation of the aorta. The subclavian and common carotid arteries are often affected bilaterally and over long segments [Figure 9]. Enhancement of the thickened walls is frequently seen on the post-contrast scans due to inflammation.<sup>[42,43]</sup>

### Medium vessel vasculitis

Polyarteritis nodosa is an immune complex vasculitis that can involve any organ system, except the lung and spleen. Vasculitic changes consist of focal, segmental inflammation

with an infiltrate of polymorphonuclear neutrophils and fibrinoid necrosis. Thrombotic occlusion leads to ischemic damage to the peripheral nerves that are involved over half of the patients. CNS involvement is seen in 20–40% of the patients. Cerebral ischemia and parenchymal hemorrhage can result from direct involvement of the cerebral vasculature or indirectly as a result of hypertension or cardiogenic embolism. CTA/DSA may reveal multiple intracranial aneurysms and stenosis/occlusion of the vessels.<sup>[44,45]</sup>

Kawasaki disease is an acute disorder occurring predominantly in children (<5 years of age) that is presumed to be caused by an unidentified infectious agent. The peak incidence of the vasculopathy is around 1–2 years of age,



**Figure 9:** A 59-year-old male patient with Takayasu arteritis. Contrast-enhanced MRA of the neck shows marked long segment narrowing of the common carotid arteries (arrows). There is severe narrowing of the left subclavian artery (curved arrow) with retrograde filling of the left vertebral artery (arrowhead) by the right vertebral artery “subclavian steal syndrome.”

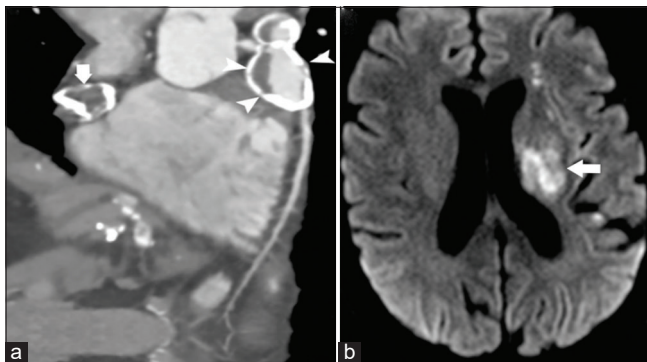


**Figure 10:** A 26-year-old male patient with Kawasaki disease presented with acute weakness on right side. (a) Coronal image of CT coronary angiogram shows large partially calcified aneurysms from the right (arrowhead) and left (arrow) coronary arteries. (b) Axial DWI image shows infarctions (arrow) in the left periventricular white matter.

and although rare, many case of adult onset of disease has been documented in literature ranging from the second to fourth decade.<sup>[46]</sup> It causes vasculopathies mostly in the form of coronary artery aneurysms and in the aorta. Coronary artery may show mild dilatation to frank aneurysm [Figure 10a and b]. Involvement of carotid arteries is rare. CNS presentation may include small lacunar infarctions or subdural/SAH, cerebral atrophy, and reversible T2 hyperintensity in the splenium of the corpus callosum.<sup>[47,48]</sup>

### Small vessel vasculitis

Wegener’s granulomatosis is a systemic vasculitis affecting small- and medium-sized arteries, arterioles, and venules primarily in the upper airways, lungs, and kidneys. About 4% of these patients show cerebrovascular events causing anterior and posterior circulation ischemic strokes as well as parenchymal and/or SAH.<sup>[45,49]</sup> Ischemic stroke has been occasionally reported as the initial manifestation of this disease.

### PRIMARY CNS VASCULITIS (PRIMARY ANGIITIS OF THE NERVOUS SYSTEM)

PACNS is an autoimmune vasculitis that exclusively involves CNS blood vessels, including the brain and spinal cord, in the absence of an underlying systemic disease.<sup>[45]</sup> Patients may present with headaches, TIAs, ischemic stroke, seizures, movement disorder, optic neuritis, or progressive cognitive decline or multifocal myelopathies with spinal cord involvement.

Small- and medium-sized blood vessels of leptomeninges and superficial cortical arteries of 200–300  $\mu\text{m}$  diameter are commonly affected.<sup>[50]</sup> Vessels show transmural infiltrate of lymphocytes, multinucleated giant cells, and segmental granulomatous changes, leading to significant intimal thickening.

Clinical diagnosis of PACNS is very challenging due to non-specific clinical features. Although conventional angiogram is considered the gold standard, because of its invasive nature, it is less frequently performed than CTA/MRA as an initial investigation. Like any other vasculitis, T2 WI shows nonspecific features of multiple ischemic microinfarcts involving the cortical or deep gray matter, or the subcortical white matter.<sup>[51]</sup> Discrete foci of acute or chronic, cortical or subcortical hemorrhages are commonly identified on GRE/SWI images. High-resolution contrast-enhanced T1 WI may show vessel wall enhancement. Conventional angiogram and to a lesser extent, CTA and MRA may show the “beads on a chain” appearance suggestive of focal segmental narrowing stenosis with normal caliber vessel [Figure 11a and b]. Unfortunately, this sign on angiography is neither absolutely sensitive nor specific for PACNS.<sup>[52,53]</sup>

## RCVS

RCVS represents a group of diverse disorders characterized by unique clinical and radiological findings with the imaging hallmark being reversible segmental vasoconstriction. This presents clinically more commonly in women, than in men, with severe thunderclap headache.<sup>[54,55]</sup> RCVS affects a wide range of demographics and races. The mean age of presentation is around 42–45 years, though other age groups, including children and older patients, can be affected. Although RCVS has been associated with numerous conditions, including pregnancy migraine, medications including vasoconstrictive drugs, no strong causal relationship has yet been established. The individual risk factors, triggers, and conditions associated with RCVS are not related and there seems to be no consensus regarding the pathogenesis of the disease. The pathophysiology is not well documented. However, it is agreed that cerebral vascular tone is altered in RCVS without pathologic changes in vascular walls. Many studies with single variables have been published to differentiate RCVS from PACNS with limited utility and applicability. In 2016, Singhal *et al.* proposed a set of criteria to diagnose RCVS and to differentiate it from PACNS with a specificity of 98–100% and a similarly high positive predictive value. This included recurrent thunderclap headaches or; single thunderclap headache with either normal neuroimaging study or; no thunderclap headache but abnormal angiographic findings with a normal neuroimaging study. The latter basically rules out PACNS which almost always has positive neuroimaging findings. PRES can occur as a complication of RCVS, and delayed vasoconstriction can occur as a consequence of PRES. Although PRES and RCVS have a bidirectional association with each other, they are not basically simultaneous.<sup>[56-58]</sup> Imaging findings include convexity SAH in a non-aneurysmal pattern, lobar pattern parenchymal hemorrhage, and watershed infarcts. There might be no visible vasoconstriction,

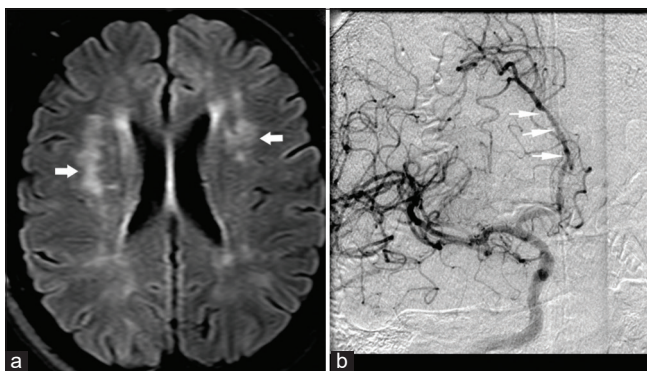


**Figure 11:** A 39-year-old female patient with CNS vasculitis presented with multiple transient ischemic attacks. (a) Axial FLAIR image shows multiple hyperintensities (arrows) in the cerebral white matter bilaterally. (b) Conventional angiogram of the brain shows multiple segmental narrowing of ACAs (arrows).

especially during the early course of disease, as the condition starts distally in vessels that are not well visualized. Angiogram (CTA/MRA, catheter) shows varying degree of segmental vasoconstriction with smooth narrowing of the large- to medium-sized arteries followed by focally dilated distal cortical branches [Figure 12a-d]. High-resolution MR VWI can help differentiate RCVS from vasculitides. There is usually none to minimal enhancement of the vessel wall as compared to intense circumferential enhancement seen in other vasculitis. The imaging findings in RCVS show complete reversal within 3–6 months of onset, which is one of the important diagnostic criteria for this condition.<sup>[54-55]</sup>

## VASCULITIS ASSOCIATED WITH SYSTEMIC DISEASE

Various connective tissue disorders such as systemic lupus erythematosus (SLE), scleroderma, rheumatoid arthritis, Sjogren syndrome, mixed connective tissue disease, and Behcet disease can involve vessels. Vessel wall involvement in most of these diseases is thought to be autoimmune.

SLE is an autoimmune disease that leads to chronic inflammation of the brain parenchyma and vessels. The prevalence of CNS involvement is approximately 30–40%. Clinical features include headaches, seizures, psychosis, cognitive decline, chorea, and neuropathies. Cerebral ischemia and infarction in SLE could be due to a variety of

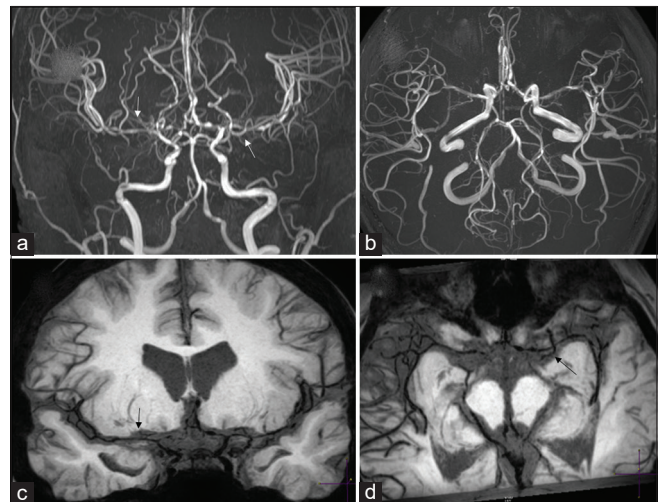


**Figure 12:** Reversible cerebral vasoconstriction syndrome (RCVS). A 32-year-old female patient with non-aneurysmal pattern subarachnoid hemorrhage on CT. (a and b) Routine MR angiogram images moderate multifocal narrowing of bilateral ACAs, MCAs with beaded appearance of distal cortical branches (arrows). (c and d) High-resolution vessel wall imaging better delineates the segmental vasoconstriction seen on MRA (arrows). There was complete resolution of narrowing on the follow-up MRA done 2 months later (not shown here).

potential mechanisms including cardiogenic embolism, lupus anticoagulant or anticardiolipin antibodies, hyperhomocysteinemia, and dissection.<sup>[59]</sup>

MRI often shows discrete focal lesions of cortical and subcortical infarcts often caused by abnormalities of coagulation and cardiac origin embolism. FLAIR and T2 WI may also show lacunar infarcts, watershed infarcts or diffuse hyperintense lesions within the deep white matter which are thought to be due to marked endothelial hyperplasia and obliterative intimal fibrosis in the small vessels of the brain, leading to occlusion, a process described as lupus angiitis or vasculitis. In addition, SLE patients may also present with dural sinus or deep venous thrombosis, especially in patients with antiphospholipid antibodies syndrome. Intracranial hemorrhage as SLE presentation may be seen in patients with uremia, thrombocytopenia, and hypertension.<sup>[60]</sup>

### CEREBRAL AUTOSOMAL DOMINANT ARTERIOPATHY WITH SUBCORTICAL INFARCTS AND LEUKOENCEPHALOPATHY (CADASIL)

CADASIL is autosomal dominant mutation caused by point mutations or small deletions in the *Notch 3* gene on chromosome 19p13.58. It usually affects middle-aged people without history of diabetes and hypertension. The four major symptoms seen in CADASIL include migraine with aura (20–40%), ischemic attacks (transient or strokes) (70–80%), psychiatric findings, and dementia (30–50%).<sup>[61]</sup>

Histopathology reveals thickened and granular osmiophilic material, PAS-positive material, which replaces smooth muscle cells of the media and weakens the vessel wall.<sup>[62]</sup> This leads to duplication and splitting of the internal elastic lamina, hypertrophy of the media, and fibrosis of medium size vessels.

On MR, T2 hyperintense lesions in the subcortical and deep white matter due to lacunar infarction are commonly seen in CADASIL. T2 hyperintensities in bilateral anterior temporal lobes and external capsules are a pathognomonic radiographic appearance in the appropriate clinical setting [Figure 13a and b]. Symmetric, confluent T2 hyperintense lesions may also be seen in insula, periventricular regions, centrum semiovale, basal ganglia, and brain stem. In the later stages, there is diffuse leukoencephalopathy, ex vacuo hydrocephalus, and brain atrophy.<sup>[61,62]</sup>

#### Sickle cell disease (SCD)

Vascular changes in SCD have four angiographic manifestations: Proximal arterial occlusion/stenosis, distal branch occlusion secondary to thrombosis or embolism, Moyamoya syndrome, and aneurysm. These changes are

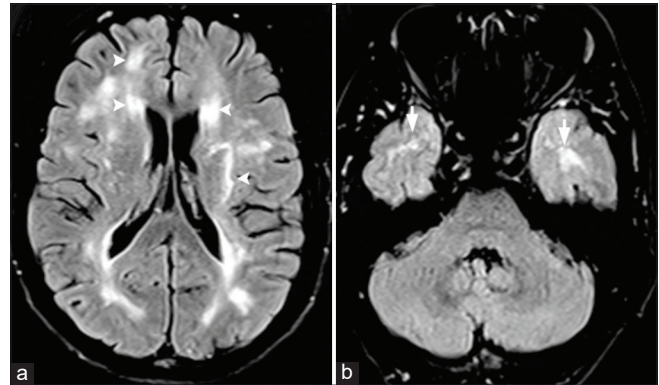


**Figure 13:** CADASIL in a 43-year-old male patient with a history of migraine and multiple transient ischemic attacks. (a) Axial FLAIR images shows patchy hyperintensities (arrowheads) scattered throughout the supratentorial white matter bilaterally. (b) Axial FLAIR image shows classical hyperintensities in the anterior aspect of the temporal lobes (arrows).

believed to be caused by damage to the intima from high-velocity blood flow, the abnormal shape of the sickle cells due to polymerization, adherence of repeated red blood cells (RBCs) to the endothelium, endothelial damage, intravascular sludge, intimal hyperplasia, and thrombosis.<sup>[63]</sup>

The incidence of brain infarction is approximately 25% and is the most severe and common complications of SCD. Stenosis of the distal intracranial ICA and proximal MCA is more common than extracranial ICA stenosis.<sup>[64,65]</sup> Intracranial velocities on Doppler >170–200 cm/sec indicate significant risk for infarction and are shown to correlate with areas of MR imaging abnormality and vessel narrowing. SCD vasculopathy may present with Moyamoya pattern progressive stenosis and occlusion of the distal ICAs and their branches. The clinical manifestations of stroke and TIAs can, however, be reduced with RBC transfusions.<sup>[66,67]</sup> Endothelial damage may also lead to aneurysm formation which is often multiple and seen mostly originate from the vertebrobasilar system. Aneurysms may manifest with subarachnoid or intraparenchymal hemorrhage. Evaluation of intracranial vessels can be done utilizing CT angiogram or TOF MR angiogram, with the latter being the modality of choice in the pediatric age group secondary to radiation concerns with CT. However, given the high flow velocities in SCD, there can be artifactual loss of flow signal at the branch points, like the carotid terminus or the tortuous cavernous segments. Contrast-enhanced MR angiogram can overcome this limitation and is now often used, especially given the fact that these segments are commonly involved in SCD.

#### Moyamoya

Moyamoya vasculopathy is a non-atherosclerotic, non-inflammatory, vasculopathy characterized by chronic

progressive stenosis or occlusion of the cerebral vasculature with particular involvement of the circle of Willis and the arteries that feed it.<sup>[68]</sup> This progressive stenosis of the arteries around the circle of Willis leads to abnormal collateral vessels at the base of the brain which is described as Moyamoya (=puff of smoke) in Japanese.<sup>[69]</sup> Moyamoya vasculopathy secondary to associated conditions is categorized as Moyamoya syndrome. Moyamoya may be classified depending on the cause [Table 3].

Pathologically, Moyamoya disease is characterized by proliferating intima with lipid deposits and fibrocellular thickening of the intima, waving of the internal elastic lamina, and thinning of the media. The exact pathogenesis of Moyamoya vasculopathy has been a subject of debate. Although there is definite evidence of the involvement of inflammatory proteins, this has historically not been recognized as a causative factor. Clinical signs and symptoms are mostly related to either cerebral ischemia or hemorrhage. Ischemic stroke is more common in younger patients while parenchymal hemorrhage being more frequent in older individuals.<sup>[70]</sup> MR brain may show multiple tiny dilated vessels in the region of deep gray matter nuclei which represent deep perforating collaterals, with various small and medium size areas of infarctions in the cerebral parenchyma. There may be scattered foci of micro- or macrohemorrhages. CTA/MRA of head shows stenosis or occlusion of distal ICAs and/or proximal portions of the middle and/or anterior cerebral arteries combined with an abundance of dilated, thin-walled collateral branches of the circle of Willis. A fine network of vessels at the base of the brain is seen as hazy, puff of smoke appearance. As the middle and anterior cerebral arteries become affected, there is a development of leptomeningeal, extracranial, transdural, and transosseous collaterals [Figure 14]. Prominent leptomeningeal collaterals result in high signal on FLAIR images due to slow flow, referred to as “ivy sign” giving the appearance of brain being covered with ivy [Figure 15 a-f]. This predicts good collateral status and better clinical outcome. Patients with Moyamoya vasculopathy may show rapid reduction in the diameter of the proximal ICA compared to the adjacent common carotid artery, giving the appearance of a champagne bottle neck. Perfusion studies may show severe decrease in the blood flow throughout the supratentorial white matter with increase in the mean transit time.<sup>[71]</sup>

**Infection-associated vasculitis**

Various organisms can cause CNS vasculitis either by primary or secondary damage to the vessels. CNS vasculitis can be due to organisms directly infecting the vessel wall or damage to blood vessels as they traverse purulent exudate in cisterns and along the cerebritis bed. Secondary vessel damage could be due to post-infectious inflammatory toxins such as

**Table 3:** Causes of Moyamoya.

1. Primary Moyamoya or “Moyamoya disease”
2. Secondary Moyamoya syndrome
  - a. Congenital disorders
    - Neurofibromatosis type 1
    - Tuberous sclerosis
    - Sickle cell anemia
    - Alpert syndrome
    - Marfan syndrome
    - Fanconi anemia
    - Down syndrome
  - b. Acquired diseases
    - Vasculitis
    - Infection
    - Thrombosis
    - Atherosclerosis
    - Trauma
    - Post-radiation arteriopathy

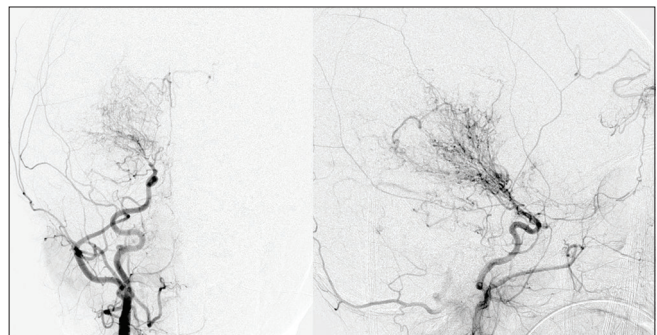


**Figure 14:** Moyamoya in a 28-year-old male patient with sickle cell disease. Frontal view of the conventional angiogram of the head shows severe narrowing of the right internal carotid artery (arrowhead) with puff of smoke (arrow) due to lenticulostriate collaterals. Multiple extracranial, transdural, and intracranial (curved arrows) collaterals are seen on the surface of the brain.

immunoglobulin, complement, lipoprotein, viral antigen or immune complex deposition, cold agglutinin formation, or vascular endothelial cell proliferation leading to vessel damage.

Bacterial, viral, tubercular, and fungal are all known to cause vasculitis and cerebrovascular events. Blood vessels traversing through the thick gelatinous basilar, bacterial, fungal, or tubercular exudate can develop inflammation, particularly in small- and medium-sized arteries.<sup>[72,73]</sup> Inflammation may lead to reactive subendothelial cells proliferation and stenosis of the vascular lumina, leading to large and small vessel thrombosis, cerebral infarction [Figure 16], and mycotic aneurysm.

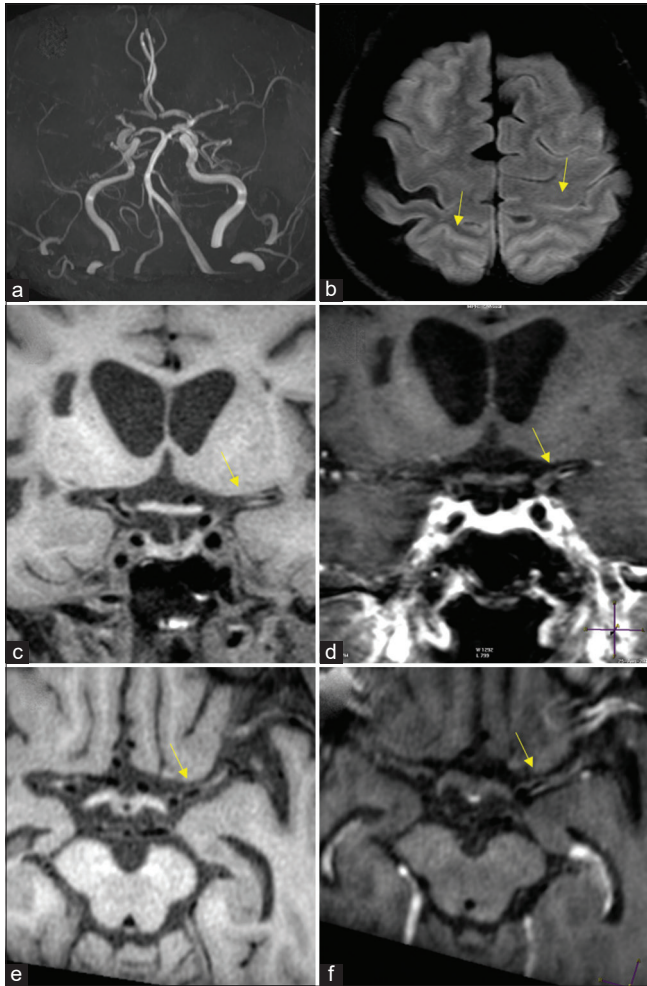


**Figure 15:** Moyamoya in a 27-year-old female patient with sickle cell disease. (a) Frontal view of the conventional angiogram of the head shows severe narrowing of the carotid terminus, more prominent on the right. (b) Axial FLAIR image reveals bright signal within the sulcal vessels suggesting collateral flow (ivy sign: Yellow arrows). Coronal (c,d) and axial (e,f) vessel wall images show concentric wall thickening of bilateral carotid terminus and left proximal MCA. Wall enhancement along on the left MCA (yellow arrows).

MRI may show meningeal inflammatory changes as hyperintense signal intensity in the basal cisterns and subarachnoid space on FLAIR. Gd-enhanced MRI will show thick enhancement in the corresponding sites. DWI may show changes of cerebritis, abscess formation, and associated acute brain infarction [Figure 17a and b]. Vascular narrowing or occlusion may be documented with standard MR sequences or by MRA.

Viruses, especially the herpes zoster, are a well-known documented cause of the viral arteritides.<sup>[74]</sup> The most common clinical symptoms of herpes vasculitis is delayed brain infarction. Focal or long segment stenosis or multifocal narrowing may be seen of the small or large arteries on MRA.<sup>[75]</sup>

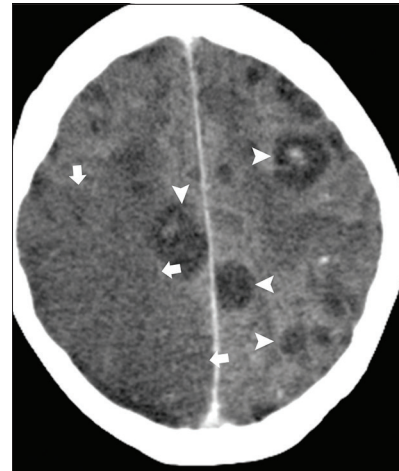


**Figure 16:** Acute infarction in a 36-year-old immunocompromised patient with aspergillosis. Axial contrast-enhanced CT images show multiple hypodense granulomas (arrowheads). Wedge shape hypodensity is seen in the right parietal lobe (arrows) consistent with acute infarction due to fungal vasculitis.

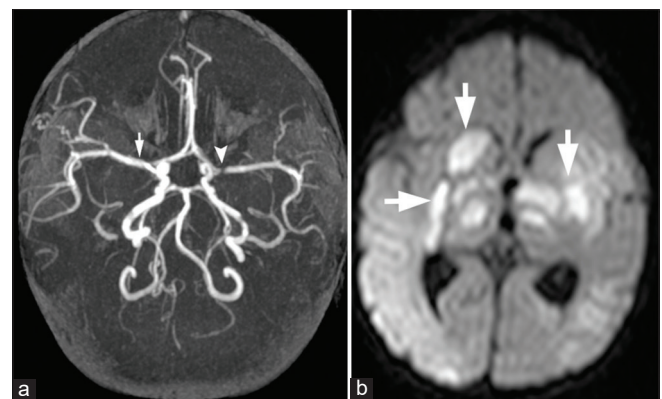


**Figure 17:** A 2-year-old child with bacterial meningitis presented with acute weakness and involuntary movements. (a) Maximum intensity projection from time-of-flight head MRA shows severe narrowing of the left M1 segment (arrowhead) and mild spasm of the right M1 segment (arrow) of MCAs. (b) Axial DWI image shows infarctions (arrows) in the bilateral deep gray matter nuclei and thalami secondary to infective vasculitis and spasm.

### Radiation-induced vasculitis

Radiation-induced vasculitis is a rare, but well-documented complication in patients with a history of previous head and neck or mediastinal radiation. RT-induced vascular disease is an acceleration of the atherosclerotic process probably due to endothelial cell damage, fibrosis of the intima-media layer, and development of atheromatous plaques.<sup>[76]</sup>

On CT and MR imaging, arteritis may be seen as thickening and enhancement of the arterial wall. In the neck, RT-induced carotid artery lesions are long segments and are not confined to the bifurcation, as in atherosclerosis. In

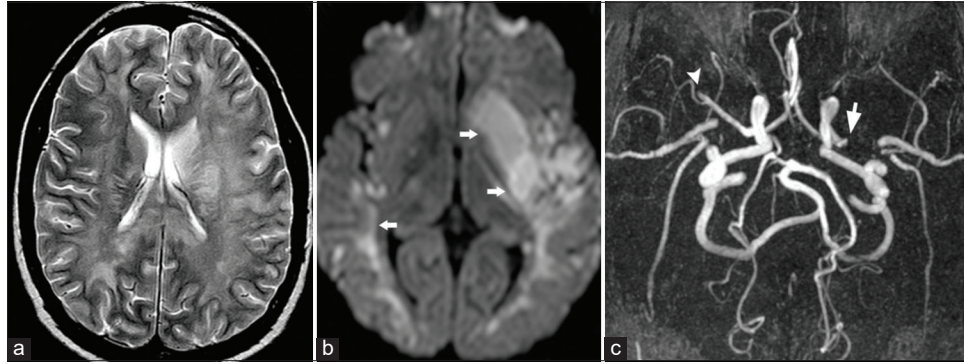


**Figure 18:** Cocaine vasculitis. A 31-year-old male patient presented to ER with acute-onset right-sided weakness. (a) Axial T2 image shows diffuse white matter hyperintensity due to vasculopathic changes. (b) Axial DWI image shows acute infarction (arrows) involving the left putamen and bilateral temporal lobe. (c) Time-of-flight MRA maximum intensity projection (MIP) shows acute cutoff of the left (arrow) and right (arrowhead) MCAs.

the brain, radiation-induced white matter changes are due to combination of vessel wall endothelial damage and detrimental effect on oligodendrocytes. Besides white matter T2 hyperintensities, multiple microhemorrhages are frequently seen on GRE /SWI images.<sup>[76,77]</sup>

### Vasculopathy in drug abusers

The CNS is a target organ for many of the prescribed medications and drugs of abuse. Drug abuse has become an important cause of stroke in adolescents and young adults. Drugs of abuse commonly affecting the CNS include cocaine, heroin, alcohol, amphetamines, toluene, and cannabis. The CNS complications include neurovascular complications, leading to stroke, hemorrhage, encephalopathy, atrophy, and secondary infection.

CNS complications in cocaine abusers mainly include ischemic stroke, parenchymal hemorrhage, and SAH. Infarcts are thought to be due direct vasospasm, enhanced platelet aggregation, cardioembolic sources, accelerated atherosclerosis, and cerebral vasculitis.<sup>[78,79]</sup> Arterial constrictions are predominantly seen in the MCAs and PCAs following IV cocaine use. For unknown reasons, there is also a higher incidence of aneurysms and vascular malformations in cocaine addicts. On MR, acute stroke which is often multifactorial is identified on DWI, on the background of chronic diffuse white matter vasculopathic changes [Figure 18a-c].

Heroin also causes ischemia and stroke primarily due to vasospasm, vasculitis, or embolic events. Heroin-induced ischemia is due to direct effects of reversible vasospasm from stimulation of vascular smooth muscle, vasculitis secondary to an immune-mediated response, and embolic effects from crystalline impure additives.<sup>[80]</sup> RCVS now encompasses what was previously thought to be a group of distinct clinical entities, including drug-induced angiopathy (vasculopathy), drug-induced cerebral arteritis as the clinical and radiological manifestations are similar.

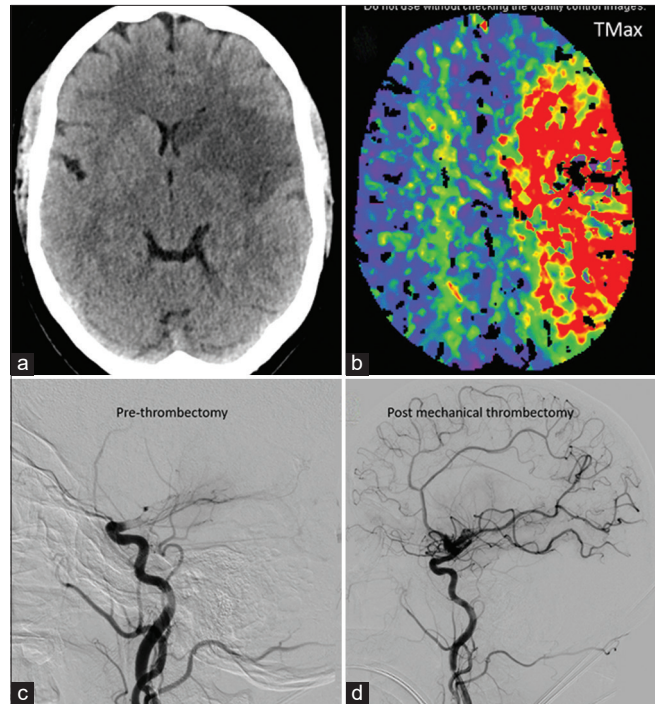


**Figure 19:** A 41-year-old COVID-positive patient with ischemic stroke secondary to large vessel occlusion: Moderate size acute infarct in the left MCA territory on non-contrast head CT (a). Large ischemic penumbra noted on the Tmax perfusion maps involving the entire left MCA territory (b). Catheter angiogram shows complete occlusion beyond the carotid terminus (c) with significant revascularization post-thrombectomy (d).

## CORONAVIRUS DISEASE 2019 (COVID-19) VASCULOPATHY

### COVID-19

COVID-19 secondary to severe acute respiratory syndrome-coronavirus-2 was declared a global pandemic on March 1, 2020. Although this primary affects the respiratory system,

it is now well established that this is a multisystem disease with widespread cases of cardiac, renal, and neurological complications. The most common neurological presentation reported, has been ischemic stroke, secondary to arterial or venous thrombosis, because of the hypercoagulable state associated with COVID-19. However, the neurological manifestations can be quite variable ranging from reversible mild demyelination to severe necrotizing encephalopathy. The virus is known to directly affect the endothelial cells through ACE2 receptors. The hypoxic status in COVID results in activation of hypoxia inducible transcription factors and downregulation of natural anticoagulants. The sum total effect is endothelial dysfunction, leading to increased blood clotting factors and a procoagulant phenotype. The affected

patients are more commonly males, generally in the sixth decade of life (mean age varying between 62 and 69 years between studies). However, smaller case series of large vessel stroke in younger patients have also been reported. Hemorrhagic stroke including SAH and hemorrhagic conversion of ischemic stroke is significantly less common. Ischemic stroke is usually secondary to large vessel occlusions, involving the cervical ICA, intracranial ICA, vertebrobasilar arteries, and proximal MCAs [Figure 19a-d]. Few cases of CNS vasculitis have also been reported, however, as the focus is usually on clinical stabilization, the threshold for performing imaging studies is high and definitive diagnosis can often not be made.<sup>[81,82]</sup>

**Table 4:** Imaging pearls to the diagnosis of common non-atherosclerotic vasculitis.

Disease process	Diagnostic pearls
Arterial dissections	CTA: Narrow eccentric lumen with an increase of the external diameter of the artery. MR: Enlarged vessel with intramural hematoma with semilunar shaped intramural hematoma.
Fibromuscular dysplasia Dolichoectasia	CTA/MRA: String of beads appearance on arteriography CT: Tortuous, slightly hyperdense, elongated vertebrobasilar artery MR: Tortuous, dilated, lateral deviation of the vessel with mass effect on brain parenchyma and cranial nerves.
Cerebral amyloid angiopathy	Elderly patient with microhemorrhages in the cortical-subcortical region with diffuse white matter T2 hyperintensity
Ehlers-Danlos syndrome	Clinical examination: Skin hyperextensibility, fragile and soft skin, delayed wound healing, easy bruising, and generalized joint hypermobility and; family history
Marfan's syndrome	Clinical manifestations involving the ocular, skeletal, and cardiovascular systems
Giant cell arteritis	Headache, blindness, ESR>100 mm/h, severe irregularities, narrowing and stenosis of the vertebral, internal and external carotid arteries.
Takayasu arteritis	CT MRI and MRA demonstrate mural thickening, long segment luminal narrowing of the subclavian and common carotid arteries
Polyarteritis Nodosa	CTA/DSA may reveal multiple extra- and intracranial aneurysms and stenosis/occlusion of the vessels
Kawasaki disease Primary angiitis of CNS	children (<5 years of age), coronary artery aneurysms Diagnosis usually by exclusion and on pathology. CTA and MRA may show the “beads on a chain” appearance suggestive of focal segmental narrowing stenosis with normal caliber vessel
Systemic lupus erythematosus	Clinical and laboratory findings with lacunar infarcts, watershed infarcts, or diffuse hypertensive lesions within the deep white matter. Arterial and venous occlusions
CADASIL	Autosomal dominant, middle-aged patient with migraine with aura, ischemic attacks (transient or strokes), psychiatric findings, and dementia (30–50%)
Sickle cell disease	Four angiographic manifestations: proximal arterial occlusion/stenosis, distal branch occlusion secondary to thrombosis or embolism, Moyamoya syndrome, and aneurysm
Infection-associated vasculitis	Underlying bacterial or fungal infection with basal exudates with vascular stenosis or narrowing due to spasm
Radiation-induced vasculitis	History of radiation with vascular narrowing and white matter changes of leukoencephalopathy
Reversible cerebral vasoconstriction syndrome (includes drug-induced vasculopathy)	Varying degree of segmental vasoconstriction with smooth narrowing of the large to medium-sized arteries. Complete reversal within 3–6 months of onset

CTA: Computed tomography angiography, MRA: Magnetic resonance angiography, CT: Computed tomography, ESR: Erythrocyte sedimentation rate, DSA: Digital subtraction angiography, CNS: Central nervous system, CADASIL: Cerebral autosomal dominant arteriopathy with subcortical infarcts and leukoencephalopathy

## CONCLUSION

NAV disorders can affect all the age groups and may present with variety of neurological symptoms such as headache, neck pain, visual symptoms, hemorrhagic and non-hemorrhagic strokes, mono or hemiplegia, or myelopathy. It also accounts for 15% of strokes in adults and 20–25% of strokes in pediatrics. It may result from various systemic or local etiologies which include collagenopathies, immunological, hematological, hereditary, infectious mechanisms, and idiopathic causes. The clinical presentations together with the imaging findings are crucial for diagnosis of this condition. Role of imaging is both determining the cause and the effects of this diverse group of diseases on vessels and brain parenchyma. Specific imaging findings and “pearls” to their diagnosis are highlighted in Table 4.

### Declaration of patient consent

Patient's consent not required as patients identity is not disclosed or compromised.

### Financial support and sponsorship

Nil.

### Conflicts of interest

There are no conflicts of interest.

## REFERENCES

1. Simma B, Martin G, Müller T, Huemer M. Risk factors for pediatric stroke: Consequences for therapy and quality of life. *Pediatr Neurol* 2007;37:121-6.
2. Schievink WI. Spontaneous dissection of the carotid and vertebral arteries. *N Engl J Med* 2001;344:898-906.
3. Leys D, Lucas C, Gobert M, Deklunder G, Pruvo JP. Cervical artery dissections. *Eur Neurol* 1997;37:3-12.
4. Barinagarrementeria F, Amaya LE, Cantu C. Causes and mechanisms of cerebellar infarction in young patients. *Stroke* 1997;28:2400-4.
5. Arnold M, Bousser MG, Fahrni G, Fischer U, Georgiadis D, Gandjour J, et al. Vertebral artery dissection: Presenting findings and predictors of outcome. *Stroke* 2006;37:2499-503.
6. Schievink WI, Mokri B, Piepgras DG. Spontaneous dissection of cervicocephalic arteries in childhood and adolescence. *Neurology* 1994;44:1607-12.
7. Muller BT, Luther B, Hort W, Neumann-Haefelin T, Aulich A, Sandmann W. Surgical treatment of 50 carotid dissections: Indications and results. *J Vasc Surg* 2000;31:980-8.
8. de Bray JM, Baumgartner RW. History of spontaneous dissection of the cervical carotid artery. *Arch Neurol* 2005;62:1168-70.
9. Dziewas R, Konrad C, Drager B, Evers S, Besselmann M, Lüdemann P, et al. Cervical artery dissection: Clinical features, risk factors, therapy and outcome in 126 patients. *J Neurol* 2003;250:1179-84.
10. Kim BM, Kim SH, Kim DI, Shin YS, Suh SH, Kim DJ, et al. Outcomes and prognostic factors of intracranial unruptured vertebral artery dissection. *Neurology* 2011;76:1735-41.
11. Kwon JY, Kim NY, Suh DC, Kang DW, Kwon SU, Kim JS, et al. Intracranial and extracranial arterial dissection presenting with ischemic stroke: Lesion location and stroke mechanism. *J Neurol Sci* 2015;358:371-6.
12. Provenzale JM, Morgenlander JC, Gress D. Spontaneous vertebral dissection: Clinical, conventional angiographic, CT, and MR findings. *J Comput Assist Tomogr* 1996;20:185-93.
13. Leclerc X, Godefroy O, Salhi A, Lucas C, Leys D, Pruvo JP. Helical CT for the diagnosis of extracranial internal carotid artery dissection. *Stroke* 1996;27:461-6.
14. dal Pozzo G, Mascalchi M, Fonda C, Cadello M, Ronchi O, Inzitari D. Lower cranial nerve palsy due to dissection of the internal carotid artery: CT and MR imaging. *J Comput Assist Tomogr* 1989;13:989-95.
15. Mascalchi M, Bianchi MC, Mangiafico S, Ferrito G, Puglioli M, Marin E, et al. MRI and MR angiography of vertebral artery dissection. *Neuroradiology* 1997;39:329-40.
16. Levy C, Laissy JP, Raveau V, Amarenco P, Servois V, Bousser MG, et al. Carotid and vertebral artery dissections: Three-dimensional time-of-flight MR angiography and MR imaging versus conventional angiography. *Radiology* 1994;190:97-103.
17. Goldberg HI, Grossman RI, Gomori JM, Asbury AK, Bilaniuk LT, Zimmerman RA. Cervical internal carotid artery dissecting hemorrhage: Diagnosis using MR. *Radiology* 1986;158:157-61.
18. Djouhri H, Guillon B, Brunereau L, Lévy C, Bousson V, Biousse V, et al. MR angiography for the long-term follow-up of dissecting aneurysms of the extracranial internal carotid artery. *AJR Am J Roentgenol* 2000;174:1137-40.
19. Chen CJ, Tseng YC, Lee TH, Hsu HL, See LC. Multisection CT angiography compared with catheter angiography in diagnosing vertebral artery dissection. *AJNR Am J Neuroradiol* 2004;25:769-74.
20. Furie DM, Tien RD. Fibromuscular dysplasia of arteries of the head and neck: Imaging findings. *AJR Am J Roentgenol* 1994;162:1205-9.
21. Slovut DP, Olin JW. Fibromuscular dysplasia. *N Engl J Med* 2004;350:1862-71.
22. Corrin LS, Sandok BA, Houser OW. Cerebral ischemic events in patients with carotid artery fibromuscular dysplasia. *Arch Neurol* 1981;38:616-8.
23. Osborn AG, Anderson RE. Angiographic spectrum of cervical and intracranial fibromuscular dysplasia. *Stroke* 1977;8:617-26.
24. Sandok BA. Fibromuscular dysplasia of the internal carotid artery. *Neurol Clin* 1983;1:17-26.
25. Luscher TF, Lie JT, Stanson AW, Houser OW, Hollier LH, Sheps SG. Arterial fibromuscular dysplasia. *Mayo Clin Proc* 1987;62:931-52.
26. Smoker WR, Corbett JJ, Gentry LR, Keyes WD, Price MJ, McKusker S. High-resolution computed tomography of the basilar artery: 2. Vertebral artery dolichoectasia: Clinical-pathologic correlation and review. *AJNR Am J Neuroradiol* 1986;7:61-72.

27. Pico F, Labreuche J, Touboul PJ, Amarenco P. Intracranial arterial dolichoectasia and its relation with atherosclerosis and stroke subtype. *Neurology* 2003;61:1736-42.
28. Samim M, Goldstein A, Schindler J, Johnson MH. Multimodality imaging of vertebrobasilar dolichoectasia: Clinical presentations and imaging spectrum. *Radiographics* 2016;36:1129-46.
29. Vinters HV. Cerebral amyloid angiopathy: A critical review. *Stroke* 1987;18:311-24.
30. Walker DA, Broderick DE, Kotsenas AL, Rubino FA. Routine use of gradient-echo MRI to screen for cerebral amyloid angiopathy in elderly patients. *AJR Am J Roentgenol* 2004;182:1547-50.
31. Malfait F, Wenstrup RJ, de Paepe A. Clinical and genetic aspects of Ehlers-Danlos syndrome, classic type. *Genet Med* 2010;12:597-605.
32. Leier CV, Call TD, Fulkerson PK, Wooley CF. The spectrum of cardiac defects in the Ehlers-Danlos syndrome types I and III. *Ann Intern Med* 1980;92:171-8.
33. Henderson FC Sr., Austin C, Benzel E, Bolognese P, Ellenbogen R, Francomano CA, *et al.* Neurological and spinal manifestations of the Ehlers-Danlos syndromes. *Am J Med Genet C Semin Med Genet* 2017;175:195-211.
34. Schievink WI, Parisi JE, Piegras DG, Michels VV. Intracranial aneurysms in Marfan's syndrome: An autopsy study. *Neurosurgery* 1997;41:866-70.
35. Kainulainen K, Pulkkinen L, Savolainen A, Kaitila I, Peltonen L. Location on chromosome 15 of the gene defect causing Marfan syndrome. *N Engl J Med* 1990;323:935-9.
36. Wityk RJ, Zanferrari C, Oppenheimer S. Neurovascular complications of marfan syndrome: A retrospective, hospital-based study. *Stroke* 2002;33:680-4.
37. Jennette JC, Falk RJ, Bacon PA, Basu N, Cid MC, Ferrario F, *et al.* 2012 Revised international Chapel Hill consensus conference nomenclature of vasculitides. *Arthritis Rheum* 2013;65:1-11.
38. Melson MR, Weyland CM, Newman NJ, Biousse V. The diagnosis of giant cell arteritis. *Rev Neurol Dis* 2007;4:128-42.
39. Schmidt WA, Kraft HE, Vorpahl K, Völker L, Gromnica-Ihle EJ. Color duplex ultrasonography in the diagnosis of temporal arteritis. *N Engl J Med* 1997;337:1336-42.
40. Koenigkam-Santos M, Sharma P, Kalb B, Oshinski JN, Weyand CM, Goronzy JJ, *et al.* Magnetic resonance angiography in extracranial giant cell arteritis. *J Clin Rheumatol* 2011;17:306-10.
41. Johnston SL, Lock RJ, Gompels MM. Takayasu arteritis: A review. *J Clin Pathol* 2002;55:481-6.
42. Tso E, Flamm SD, White RD, Schwartzman PR, Mascha E, Hoffman GS. Takayasu arteritis: Utility and limitations of magnetic resonance imaging in diagnosis and treatment. *Arthritis Rheum* 2002;46:1634-42.
43. Choe YH, Han BK, Koh EM, Kim DK, Do YS, Lee WR. Takayasu's arteritis: Assessment of disease activity with contrast-enhanced MR imaging. *AJR Am J Roentgenol* 2000;175:505-11.
44. Rozo JC, Jefferies JL, Eidem BW, Cook PJ. Kawasaki disease in the adult: A case report and review of the literature. *Tex Heart Inst J* 2004;31:160-4.
45. Moore PM, Richardson B. Neurology of the vasculitides and connective tissue disease. *J Neurol Neurosurg Psychiatry* 1998;65:10-22.
46. Provenzale JM, Allen NB. Neuroradiologic findings in polyarteritis nodosa. *AJNR Am J Neuroradiol* 1996;17:1119.
47. Fujiwara S, Yamano T, Hattori M, Fujiseki Y, Shimada M. Asymptomatic cerebral infarction in Kawasaki disease. *Pediatr Neurol* 1992;8:235-6.
48. Okanishi T, Enoki H. Transient subcortical high-signal lesions in Kawasaki syndrome. *Pediatr Neurol* 2012;47:295-8.
49. Provenzale JM, Allen NB. Wegener granulomatosis: CT and MR findings. *AJNR Am J Neuroradiol* 1996;17:785-92.
50. Hajj-Ali RA, Calabrese LH. Primary angiitis of the central nervous system. *Autoimmun Rev* 2013;12:463-6.
51. Giannini C, Salvarani C, Hunder G, Brown RD. Primary central nervous system vasculitis: Pathology and mechanisms. *Acta Neuropathol* 2012;123:759-72.
52. Campi A, Benndorf G, Filippi M, Reganati P, Martinelli V, Terreni MR. Primary angiitis of the central nervous system: Serial MRI of brain and spinal cord. *Neuroradiology* 2001;43:599-607.
53. Ay H, Sahin G, Saatci I, Söylemezoğlu F, Saribaş O. Primary angiitis of the central nervous system and silent cortical hemorrhages. *AJNR Am J Neuroradiol* 2002;23:1561-63.
54. Miller TR, Shivashankar R, Mossa-Basha M, Gandhi D. Reversible cerebral vasoconstriction syndrome, part 1: Epidemiology, pathogenesis, and clinical course. *AJNR Am J Neuroradiol* 2015;36:1392-9.
55. Miller TR, Shivashankar R, Mossa-Basha M, Gandhi D. Reversible cerebral vasoconstriction syndrome, part 2: Diagnostic work-up, imaging evaluation, and differential diagnosis. *AJNR Am J Neuroradiol* 2015;36:1580-8.
56. Singhal AB, Topcuoglu MA, Fok JW, Kursun O, Nogueira RG, Frosch MP, *et al.* Reversible cerebral vasoconstriction syndromes and primary angiitis of the central nervous system: Clinical, imaging, and angiographic comparison. *Ann Neurol* 2016;79:882-94.
57. Choi HA, Lee MJ, Choi H, Chung CS. Characteristics and demographics of reversible cerebral vasoconstriction syndrome: A large prospective series of Korean patients. *Cephalalgia* 2018;38:765-75.
58. Obusez EC, Hui F, Hajj-Ali RA, Cerejo R, Calabrese LH, Hammad T, *et al.* High-resolution MRI vessel wall imaging: Spatial and temporal patterns of reversible cerebral vasoconstriction syndrome and central nervous system vasculitis. *AJNR Am J Neuroradiol* 2014;35:1527-32.
59. Hanly JG, Walsh NM, Sangalang V. Brain pathology in systemic lupus erythematosus. *J Rheumatol* 1992;19:732-41.
60. Futrell N, Schultz LR, Millikan C. Central nervous system disease in patients with systemic lupus erythematosus. *Neurology* 1992;42:1649-57.
61. Tournier-Lasserre E, Joutel A, Melki J, Weissenbach J, Lathrop GM, Chabriat H, *et al.* Cerebral autosomal dominant arteriopathy with subcortical infarcts and leukoencephalopathy maps to chromosome 19q12. *Nat Genet* 1993;3:256-9.
62. Ruchoux MM, Maurice CA. CADASIL: Cerebral autosomal dominant arteriopathy with subcortical infarcts and leukoencephalopathy. *J Neuropathol Exp Neurol* 1997;56:947-64.
63. Steen RG, Emudianughe T, Hankins GM, Wynn LW,

- Wang WC, Xiong X, *et al.* Brain imaging findings in pediatric patients with sickle cell disease. *Radiology* 2003;228:216-25.
64. Hirtz D, Kirkham FJ. Sickle cell disease and stroke. *Pediatr Neurol* 2019;95:34-41.
  65. Lonergan GJ, Cline DB, Abbondanzo SL. Sickle cell anemia. *Radiographics* 2001;21:971-94.
  66. Platt OS. Preventing stroke in sickle cell anemia. *N Engl J Med* 2005;353:2743-5.
  67. Verlhac S, Bernaudin F, Tortrat D, Brugieres P, Mage K, Gaston A, *et al.* Detection of cerebrovascular disease in patients with sickle cell disease using transcranial Doppler sonography: Correlation with MRI, MRA, and conventional angiography. *Pediatr Radiol* 1995;25:S14-9.
  68. Yilmaz EY, Pritz MB, Bruno A, Lopez-Yunez A, Biller J. Moyamoya: Indiana university medical center experience. *Arch Neurol* 2001;58:1274-8.
  69. Bruno A, Adams HP Jr., Biller J, Rezai K, Cornell S, Aschenbrenner CA. Cerebral infarction due to moyamoya disease in young adults. *Stroke* 1988;19:826-33.
  70. Yonekawa Y, Kahn N. Moyamoya disease. *Adv Neurol* 2003;92:113-8.
  71. Strother MK, Anderson MD, Singer RJ, Du L, Moore RD, Shyr Y, *et al.* Cerebrovascular collaterals correlate with disease severity in adult North American patients with moyamoya disease. *AJNR Am J Neuroradiol* 2014;35:1318-24.
  72. Bernaerts A, Vanhoenacker FM, Parizel PM, van Goethem JW, van Altena R, Laridon A, *et al.* Tuberculosis of the central nervous system: Overview of neuroradiological findings. *Eur Radiol* 2003;13:1876-90.
  73. Chan KH, Cheung RT, Lee R, Mak W, Ho SL. Cerebral infarcts complicating tuberculous meningitis. *Cerebrovasc Dis* 2005;19:391-5.
  74. Hilt DC, Buchholz D, Krumholz A, Weiss H, Wolinsky JS. Herpes zoster ophthalmicus and delayed contralateral hemiparesis caused by cerebral angiitis: Diagnosis and management approaches. *Ann Neurol* 1983;14:543-53.
  75. Doyle PW, Gibson G, Dolman C. Herpes zoster ophthalmicus with contralateral hemiplegia: Identification of cause. *Ann Neurol* 1983;14:84-5.
  76. Aoki S, Hayashi N, Abe O, Shirouzu I, Ishigame K, Okubo T, *et al.* Radiation-induced arteritis: Thickened wall with prominent enhancement on cranial MR images report of five cases and comparison with 18 cases of moyamoya disease. *Radiology* 2002;223:683.
  77. Bitzer M, Topka H. Progressive cerebral occlusive disease after radiation therapy. *Stroke* 1995;26:131.
  78. Fessler RD, Eshaki CM, Stankewitz RC, Johnson RR, Diaz FG. The neurovascular complications of cocaine. *Surg Neurol* 1997;47:339-45.
  79. Brown E, Prager J, Lee HY, Ramsey RG. CNS complications of cocaine abuse: Prevalence, pathophysiology, and neuroradiology. *AJR Am J Roentgenol* 1992;159:137-47.
  80. Geibprasert S, Gallucci M, Krings T. Addictive illegal drugs: Structural neuroimaging. *AJNR Am J Neuroradiol* 2010;31:803-8.
  81. Ellul M, Benjamin L, Singh B, Lant S, Michael BD, Easton A, *et al.* Neurological associations of COVID-19. *Lancet Neurol* 2020;19:767-83.
  82. Yaghi S, Ishida K, Torres J, Grory BM, Raz E, Humbert K, *et al.* SARS-CoV-2 and stroke in a New York healthcare system. *Stroke* 2020;51:2002-11.

**How to cite this article:** Agarwal A, Bathla G, Kanekar S. Imaging of non-atherosclerotic vasculopathies. *J Clin Imaging Sci* 2020;10:62.